Ann Surg Oncol (2013) 20:1676–1683
DOI 10.1245/s10434-012-2799-z

Annals of
SURGICAL ONCOLOGY
OFFICIAL JOURNAL OF THE SOCIETY OF SURGICAL ONCOLOGY

ORIGINAL ARTICLE – THORACIC ONCOLOGY

Advantages of Diffusion-Weighted Imaging Over Positron Emission Tomography-Computed Tomography in Assessment of Hilar and Mediastinal Lymph Node in Lung Cancer

Katsuo Usuda, MD[1], Motoyasu Sagawa, MD[1], Nozomu Motono, MD[1], Masakatsu Ueno, MD[1], Makoto Tanaka, MD[1], Yuichiro Machida, MD[1], Munetaka Matoba, MD[2], Yasuaki Kuginuki, MD[2], Mitsuru Taniguchi, MD[2], Yoshimichi Ueda, MD[3], and Tsutomu Sakuma, MD[1]

[1]Department of Thoracic Surgery, Kanazawa Medical University, Uchinada, Ishikawa, Japan; [2]Department of Radiology, Kanazawa Medical University, Uchinada, Ishikawa, Japan; [3]Department of Pathophysiological and Experimental Pathology, Kanazawa Medical University, Uchinada, Ishikawa, Japan

ABSTRACT

Background. The significance of diffusion-weighted imaging (DWI) is uncertain for the diagnosis of nodal involvement. The purpose of this study was to examine diagnostic capability of DWI compared with PET-CT for nodal involvement of lung cancer.

Methods. A total of 160 lung cancers (114 adenocarcinomas, 36 squamous cell carcinomas, and 10 other cell types) were analyzed in this study. DWI and PET-CT were performed preoperatively.

Results. The optimal cutoff values to diagnose metastatic lymph nodes were 1.70×10^{-3} mm^2/s for ADC value and 4.45 for SUVmax. DWI correctly diagnosed N staging in 144 carcinomas (90 %) but incorrectly diagnosed N staging in 16 (10 %) [3 (1.9 %) had overstaging, 13 (8.1 %) had understaging]. PET-CT correctly diagnosed N staging in 133 carcinomas (83.1 %) but incorrectly diagnosed N staging in 27 (16.8 %) [4 (2.5 %) had overstaging, 23 (14.4 %) had understaging]. Sensitivity, accuracy, and negative predictive value for N staging by DWI were significantly higher than those by PET-CT. Of the 705 lymph node stations examined, 61 had metastases, and 644 did not. The maximum diameter of metastatic lesions in lymph nodes were 3.0 ± 0.9 mm in 21 lymph node stations not detected by either DWI or PET-CT: 7.2 ± 4.1 mm in 39 detected by DWI, and 11.9 ± 4.1 mm in 24 detected by PET-CT. There were significant differences among them. The sensitivity (63.9 %) for metastatic lymph node stations by DWI was significantly higher than that (39.3 %) by PET-CT. The accuracy (96.2 %) for all lymph node stations by DWI was significantly higher than that (94.3 %) by PET-CT.

Conclusions. DWI has advantages over PET-CT in diagnosing malignant from benign lymph nodes of lung cancers.

Positron emission tomography (PET) has been demonstrated to be superior to CT in diagnosing nodal involvement in lung cancer, but false-positive results are not uncommon in PET.[1–4] PET-CT with 18-fluoro-2-deoxy-glucose (^{18}F-FDG) is widely accepted as an imaging modality of choice in tumor staging because of its good sensitivity.[1–4] Recently, diffusion-weighted magnetic resonance imaging (DWI) has been used to detect the restricted diffusion of water molecules. The principals of DWI exploit the random motion, or so-called Brownian movement, of water molecules in biologic tissue.[5] The primary application of DWI has been in brain imaging, mainly for the evaluation of acute ischemic stroke, intracranial tumors, and demyelinating diseases.[6–8] Diffusion of water molecules in malignant tumors is usually restricted compared to that in normal tissue, resulting in a decreased apparent diffusion coefficient (ADC) value.[9–11] In DWI, blood flow and normal tissue showing high diffusion are undetectable, but cancer tissue with low Brownian motion of water molecules is detectable. Some recent studies comparing DWI with PET-CT have shown that DWI at 1.5 T is comparable with PET-CT for detecting malignant

First Received: 6 July 2012;
Published Online: 16 December 2012

K. Usuda, MD
e-mail: usuda@kanazawa-med.ac.jp

lesions.[12–14] Furthermore, DWI was reported to be superior to PET-CT in the detection of primary lesions and the nodal assessment of non-small cell lung cancers.[15] The superiority of DWI can be explained not only by DWI giving fewer false-positive results for N staging of non-small cell lung cancer compared with PET-CT but also by DWI giving fewer false-negative results for it.[13,15] The purpose of this study was to examine the diagnostic capability of DWI compared with PET-CT in the assessment of nodal involvement of lung cancer.

PATIENTS AND METHODS

Eligibility

The study protocol for examining DWI and PET-CT in patients with pulmonary lesions was approved by the ethical committee in Kanazawa Medical University (the approval number: No. 189). Patients who had metal or pacemakers in their body or tattoos on their skin were excluded because of contraindication in MRI examinations. Informed consent was obtained from all patients after discussing the risks and benefits of the study with their surgeons.

Patients

Between May 2009 to February 2012, 158 patients who had operable lung cancer or who were highly suspected of having lung cancer were enrolled in this study. All of these patients were diagnosed with lung cancer before or during their operation. Ninety-four patients were male and 64 were female. Their mean age was 68 years (range 37–83). Two patients had double lung cancers. Cell type, pathological N factor, and metastatic lymph node station were determined by reviewing the pathological reports. There were 114 adenocarcinomas, 36 squamous cell carcinomas, 3 large cell carcinomas, 3 small cell carcinomas, 1 adenosquamous carcinoma, 1 large cell neuroendocrine carcinoma, 1 carcinoid, and 1 carcinosarcoma. TNM classification and the lymph node stations of lung cancer were classified according to the new definition of UICC 7.[16]

Open procedures were performed for 22 lung cancers, video-assisted minithoracotomies were performed for 119 lung cancers, and video-assisted thoracoscopic pulmonary resections were performed for 29 lung cancers. Patients who underwent pneumonectomies, bilobectomies, or lobectomies also underwent systematic lymphadenectomies of the hilum and mediastinal areas in video-assisted thoracoscopic pulmonary resection as well as in open procedures and video-assisted minithoracotomies. Segmentectomies or partial resections for small lung cancers with ground glass opacity (GGO) were not followed by systematic lymphadenectomies because of the lower possibility of carcinoma metastasis. There were 7 pneumonectomies, 1 bilobectomy, 119 lobectomies, 3 segmentectomy, and 30 partial resections. There were 56 pathological T1a (pT1a) carcinomas, 31 pT1b carcinomas, 39 pT2a carcinomas, 12 pT2b carcinomas, 17 pT3 carcinomas, and 5 pT4 carcinomas. There were 124 pathological pN0 (pN0) carcinomas, 20 pN1 carcinomas, and 16 pN2 carcinomas. There were 82 pathological Stage IA (pStage IA), 28 pStage IB, 14 pStageIIA, 9 pStage IIB, 19 pStage IIIA, 2 pStage IIIB, and 6 pStage IV.

MR Imaging

All MR images were obtained with a 1.5 T superconducting magnetic scanner (Magnetom Avanto; Siemens, Erlangen, Germany) with two anterior six-channel body phased-array coils and two posterior spinal clusters (six-channels each). The conventional MR images consisted of a coronal T1-weighted, spin-echo sequence [repetition time (TR) ms/echo time (TE) ms/excitations, 720/20/1) and coronal and axial T2-weighted fast spin-echo sequences (6700/130/1). DWI using a single-shot echoplanar technique were performed under spectral attenuated inversion recovery (SPAIR) with respiratory triggered scan with the following parameter: TR/TE/flip angle, 3,000–4,500/65/90; diffusion gradient encoding in three orthogonal directions; b value $= 0$ and 800 s/mm^2; receiver bandwidth, 2.442 Hz/Px; voxel size, $2.7 \times 2.7 \times 6.0$ mm; field of view, 350 mm; matrix size, 128×128; section thickness, 6 mm; section gap, 0 mm; and number of excitations, 5. One radiologist (YK) with 22 years of MRI experience who was unaware of the patients' clinical data, and one pulmonologist (KU) with 28 years of experience evaluated the MRI data. A consensus was reached if there were any differences of opinion. After image reconstruction, a two-dimensional (2D) round or elliptical region of interest (ROI) was drawn on the lesion, which was detected visually on the ADC map with reference to the T2-weighted image or CT. Areas with necrosis were excluded from the ADC measurement. The procedure was repeated three times, and the mean ADC value was obtained. A receiver operating characteristics curve (ROC curve) was constructed according to the ADC value using GraphPad Prism (Version 5.02, GraphPad Software, Inc. La Jolla, CA), and the optimal cutoff value (OCV) of the ADC value for diagnosing metastatic lymph nodes was determined. Lymph nodes with an ADC value that was equal or less than the OCV were defined as positive for malignancy. Lymph nodes with an ADC value that was higher than the OCV, or those that could not be detected on DWI, were defined as negative for malignancy.

PET-CT

PET-CT scanning was performed with a dedicated PET camera (SIEMENS Biography Sensation 16, Erlangenm Germany) before surgery. All patients fasted for 6 h before scanning. The dose of ^{18}F-FDG administered was 3.7 MBq/Kg of body weight. After a 60-min uptake period, an emission scan was acquired for 3 min per bed position and a whole-body scan was performed on each patient using several bed positions according to the height of each patient. One radiologist (MT) with 12 years of radioisotope scintigraphy and PET-CT experience who was unaware of the patients' clinical data and one pulmonologist (KU) with 28 years of experience evaluated the PET-CT data. A consensus was reached if there were any differences of opinion. After image reconstruction, a 2D round region of interest (ROI) was drawn on a slice after visual detection of the highest count on the fused CT image. Areas with necrosis were excluded from the SUV measurement. For the lesions with negative or faintly positive PET findings, the ROI was drawn on the fusion image with the corresponding CT. From those ROI, the maximum standardized uptake value (SUVmax) was calculated as the ^{18}F-FDG accumulation within lesions. A ROC curve was constructed according to the SUVmax using GraphPad Prism, and the OCV of the SUVmax for diagnosing metastatic lymph nodes was determined. Lymph nodes with a SUVmax equal or higher than the OCV were defined as positive for malignancy. Lymph nodes with a SUVmax less than the OCV or those that could not be detected on PET-CT were defined as negative for malignancy.

Measurement of the Maximum Diameter of Metastatic Lesions in Lymph Node Stations

Based on the pathological reports, all pathologic slides of metastatic lymph node stations in this series were reviewed. Microphotographs, which showed metastatic lesions in lymph nodes, were taken at an amplification of $\times$20. The maximum diameters of metastatic lesions in a lymph node station were measured three times using image analysis software (WinROOF, Mitani Corp. Japan; Fig. 1), and the longest measurement of them was used for the analysis.

Statistical Analysis

Statistical analysis was performed using StatView for Windows (Version 5.0; SAS Institute Inc. Cary, NC). The data are expressed as the mean $\pm$ SD. A two-tailed Student *t* test was used for comparison of ADC values or SUVmax in several pathological factors. The sensitivity, specificity, and accuracy of DWI versus PET-CT for pulmonary malignant and benign lesions were compared by using McNemar test. Differences of ratios between two groups were compared by using the χ^2 test. $p < 0.05$ was considered statistically significant.

RESULTS

The ROC curve for the ADC value for diagnosing metastatic lymph nodes in DWI revealed the OCV was 1.7×10^{-3} mm^2/s (Fig. 2a). The ROC curve for the SUVmax for diagnosing metastatic lymph nodes in PET-CT revealed the OCV was 4.45 (Fig. 2b). Two representative cases are presented in Figs. 3 and 4.

Concerning clinical N staging by DWI, DWI correctly diagnosed N staging in 144 carcinomas (90 %) but incorrectly diagnosed N staging in 16 (10 %) [3 (1.9 %) had overstaging, 13(8.1 %) had understaging] (Table 1). PET-CT correctly diagnosed N staging in 133 carcinomas (83.1 %) but incorrectly diagnosed N staging in 27 (16.8 %) [4 (2.5 %) had overstaging, 23(14.4 %) had understaging]. Sensitivity [63.9 % (23/36)] of N staging by DWI was significantly higher than that [36.1 % (13/36)] by PET-CT ($p = 0.0063$). Specificity [98.4 % (122/124)] for N staging by DWI was similar to that [96.8 % (120/124)] by PET-CT ($p = 0.69$). Accuracy [90.6 % (145/160)] for N staging by DWI was significantly higher than that [83.1 % (133/160)] by PET-CT ($p = 0.0095$). Positive predictive value (PPV) [75.9 % (22/29)] of DWI was not significantly higher than that [68.4 % (13/19)] of PET-CT ($p = 0.57$), and negative predictive value (NPV) [93.1 % (122/131)] of DWI was significantly higher than that [85.1 % (120/141)] of PET-CT ($p = 0.035$).

When clinical N factors by DWI were the same by PET-CT, the clinical N factors were judged as correct in 94.2 % (130/138) of carcinomas but incorrect in 5.8 % (8/138). When clinical N factors by DWI were different from those by PET-CT, clinical N factors by DWI were judged as correct in 68.2 % (15/22) of carcinomas, whereas clinical N factors by PET-CT were correct in 13.6 % (3/22); both clinical N factors by DWI of PET-CT were incorrect in 18.2 % (4/22).

Of the 705 lymph node stations examined, 61 had metastases, and 644 did not. The average value of maximum diameter of carcinomas in metastatic lymph node stations were 3.0 $\pm$ 0.9 mm (1.6–4.0 mm) in 21 lymph node stations not detected by either DWI or PET-CT (A), 7.2 $\pm$ 4.1 mm (2.1–17.0 mm) in 39 lymph node stations detected by DWI (B), and 11.9 $\pm$ 4.1 mm (6.0–17.0 mm) in 24 lymph node stations detected by PET-CT (C) (Fig. 5). The maximum diameter of group A was significantly smaller than that of group B, and that of group C,

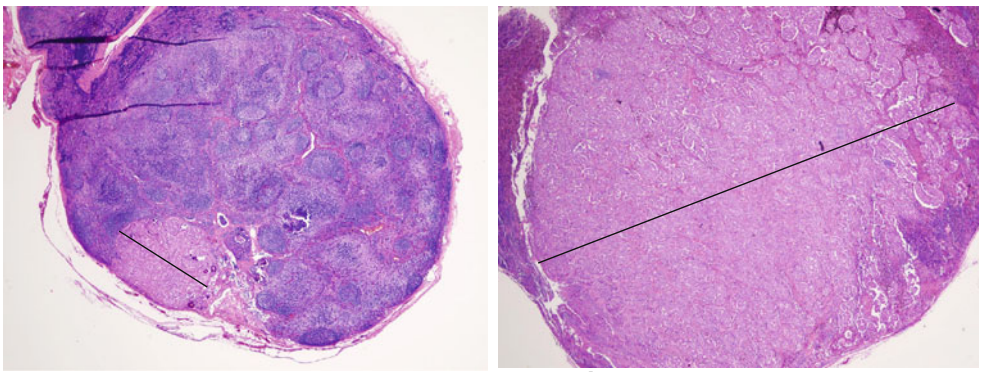

a Lymph node metastasis (#12L) **b** Lymph node metastasis (#12u)

FIG. 1 Measurement of maximum diameter of metastatic lesions in lymph node stations. **a** Tiny metastatic lesion (maximum diameter: 1.6 mm) was recognized in #12L lymph node. The metastatic lesion was not detected by DWI or by PET-CT before surgery. **b** An obvious metastatic lesion (maximum diameter: 6.8 mm) was recognized in #12u lymph node. The metastatic lesion was detected by DWI but not by PET-CT before surgery

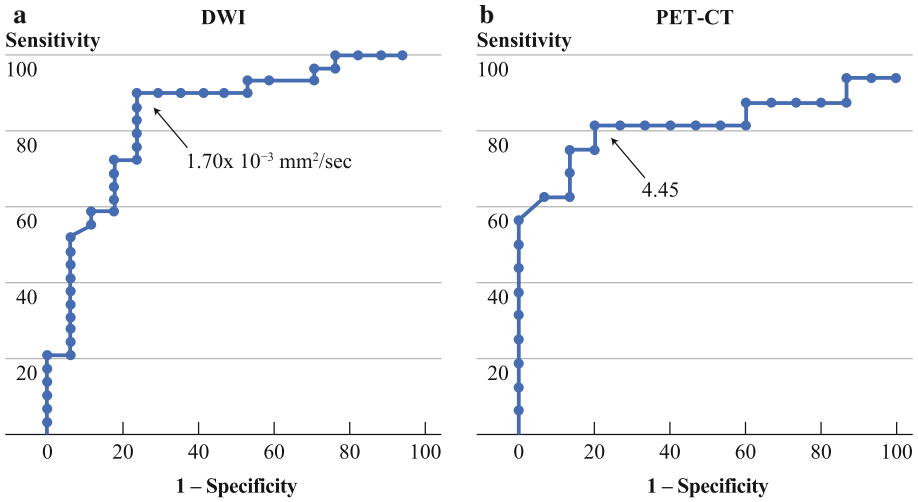

FIG. 2 **a** Receiver operating characteristic curve for the apparent diffusion coefficient value for diagnosing metastatic lymph nodes in DWI revealed that the optimal cutoff value was 1.70×10^{-3} mm^2/s. Area under the curve, 84.1 %; 95 % confidence interval, 71.8–96.4 %. Sensitivity was 89.7 % and specificity was 76.5 %. **b** Receiver operating characteristic curve for the standardized uptake value maximum for diagnosing metastatic lymph nodes in PET-CT revealed that the optimal cutoff value was 4.45. Area under the curve, 81.5 %; 95 % confidence interval, 64.9−98.1 %. Sensitivity was 81.3 % and specificity was 80 %

and the maximum size of group B was significantly smaller than that of group C. DWI detected significantly smaller size of metastatic lymph nodes than that by PET-CT in lung cancer.

In this series, there were six silicotic lesions of hilar and mediastinal lymph nodes with lung cancer. PET-CT showed moderate accumulation (4.04 ± 0.42) of FDG in the silicotic lymph nodes.

The sensitivity [63.9 % (39/61)] for metastatic lymph node stations by DWI was significantly higher than that [39.3 % (24/61)] by PET-CT ($p = 0.00027$). The specificities of DWI and PET-CT for the 644 nonmetastatic lymph node stations were 99.2 % (639/644) and 99.5 % (641/644), respectively. There was no significant difference in the specificities between DWI and PET-CT ($p = 0.73$). The accuracy [96.2 % (678/705)] for all 705 lymph node stations by DWI was significantly higher than that [94.3 % (665/705)] by PET-CT ($p = 0.015$).

DISCUSSION

PET gives false-negative results for well-differentiated pulmonary adenocarcinoma and small volumes of metabolically active tumor, and false-positive results for inflammatory nodules.[17–21] DWI can be used to distinguish benign from malignant lesions in the lung, in the thorax, in the prostate, in the breast, and in the liver.[14,22–26]

DWI has several advantages over PET-CT. First, the sensitivity and the accuracy by DWI for diagnosing

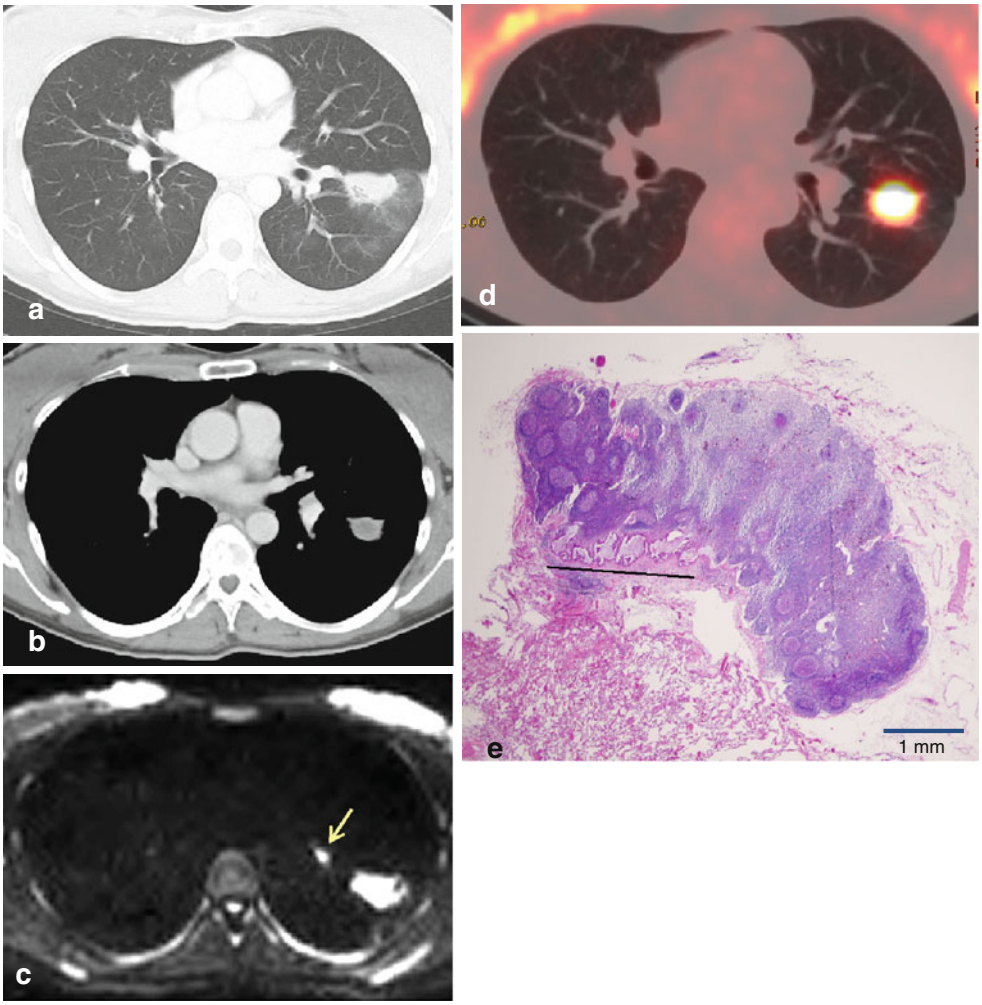

FIG. 3 Chest CT (**a**, **b**), DWI (**c**), and PET-CT (**d**) of one patient with adenocarcinoma. DWI and PET-CT identified the malignant lesion clearly. ADC value of the lung cancer was 1.239×10^{-3} mm^2/s, and its SUVmax was 11.3. A metastatic lesion (highlighted by an *arrow*; ADC value: 1.55) of a #12L lymph node was recognized by DWI but not by PET-CT before surgery. A tiny metastatic lesion (*solid line*: 2.1 mm) was detected histopathologically in a #12L lymph node (**e**)

metastatic lymph node stations were reported to be significantly higher than those by PET-CT. Nomori et al.[13] reported that the accuracy of N staging in the 88 lung cancer patients was 89 % with DWI, which was significantly higher than the value of 78 % obtained with PET-CT because of less overstaging in the former. In this study, the accuracy for N staging (90 %) by DWI was significantly higher than that (83.1 %) by PET-CT. Several reports show that understaging assessment by PET-CT is not rare in lung cancer cases.[27,28] In non-small cell lung cancers with clinical stage IA by PET-CT, 14.3 % (21/147) of them had occult nodal (N1 or N2) metastasis.[27] PET-CT staged lung cancer correctly in 128 of 159 patients (80.5 %), overstaging occurred in 9 patients (5.7 %) and understaging in 22 patients (13.8 %).[28] These data were similar to our data. In this study, the reason for more frequent false-negative results for N staging by PET-CT compared with DWI is due to tiny metastatic lesions with a maximum diameter of 6.0 mm or less in lymph nodes, which cannot be detected by PET-CT but can by DWI. Very tiny metastatic lesions whose maximum diameter was 3.0 mm or less could not detect by not only PET-CT but also DWI. This is a limitation of PET-CT and of DWI for lymph node assessment of lung cancer. Lymph nodes affected by silicosis have proven to have moderate FDG accumulation in PET-CT, which were likely to be false-positive results. DWI with ADC value and signal intensity can be useful in differentiation of malignant and benign mediastinal lymph nodes.[29]

Second, a MRI examination has easier accessibility and is relatively cheaper compared to a PET-CT examination. The cost of a DWI examination is approximately 300 US dollars which is one third of that of a PET-CT examination

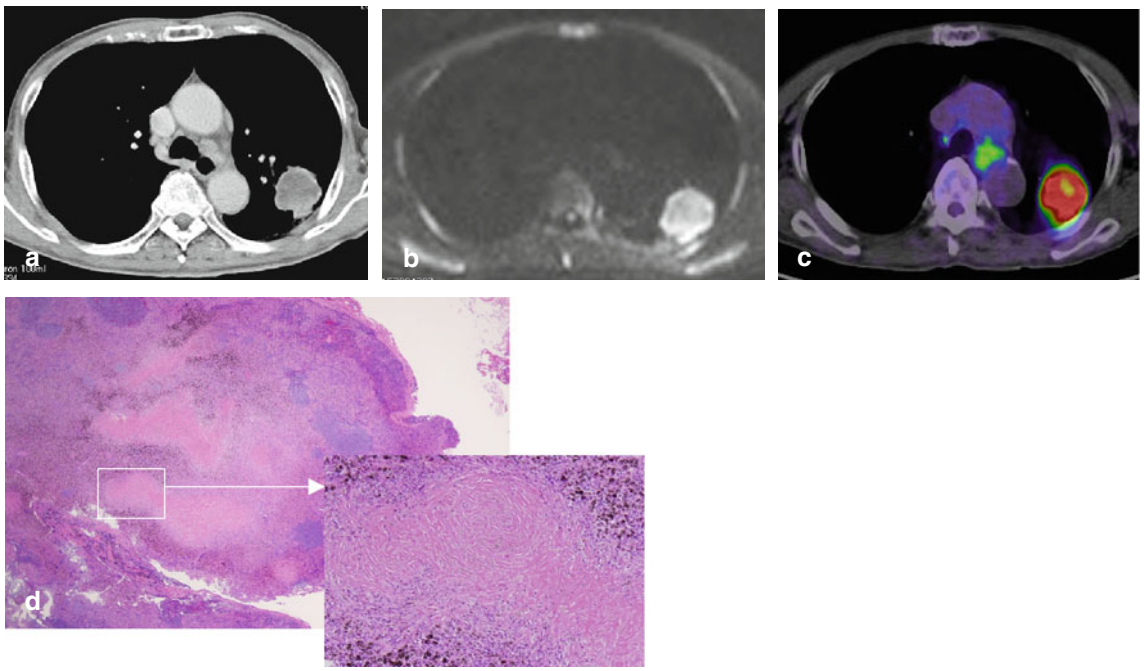

FIG. 4 Chest CT (**a**), DWI (**b**), and PET-CT (**c**) of one patient with large cell carcinoma. DWI and PET-CT identified the malignant lesion clearly. FDG accumulation (SUVmax: 4.39) in a #4L lymph node was recognized in PET-CT (**c**), but the lymph node was not recognized in DWI (**b**). Silocotic lesion was diagnosed histopathologically in the #4L lymph node (**d**)

TABLE 1 Relationships between clinical N factors by DWI or PET-CT and pathological N factors

Clinical N factor		Pathological N factor		
		pN0	pN1	pN2
DWI	cN0	122	6	3
	cN1	2	13	4
	cN2	0	1	9
PET-CT	cN0	120	13	8
	cN1	3	7	2
	cN2	1	0	6

(approximately $1,000). Hospitals equipped with PET-CT are limited because of the difficulty in handling the radioisotope of ^{18}F-FDG.

Third, in a DWI examination patients do not have to fast before the examination, do not need exogenous contrast medium, and less time is required for the examination. DWI has no risk of radiation exposure, whereas a PET-CT examination has some risk of radiation exposure.

The issue of what values should be the OCV of metastatic lymph nodes for ADC of DWI or SUVmax of PET-CT still remains. Many researchers, including us, adopted a ROC curve to determine the OCV, which were rather different from each other. For clinical convenience, a standard OCV of malignancy is necessary for ADC of DWI or SUVmax of PET-CT.

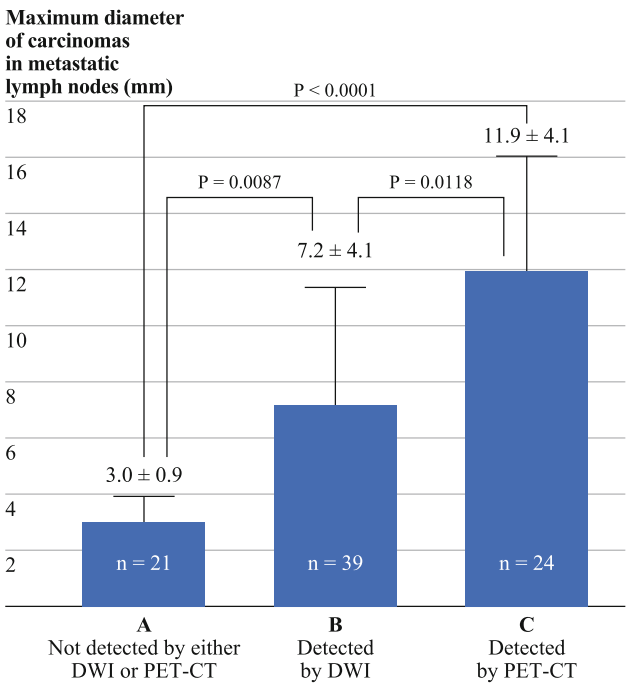

FIG. 5 The average value of maximum diameter of carcinomas in metastatic lymph node stations not detected by either DWI or PET-CT (**a**), detected by DWI (**b**), and detected by PET-CT (**c**). Maximum diameter of carcinomas in metastatic lymph node stations were 3.0 ± 0.9 mm (**a**), 7.2 ± 4.1 mm (**b**), and 11.9 ± 4.1 mm (**c**). There were significant differences among groups

We have to keep in mind that there are two important limitations of DWI. First, pulmonary lesions with histopathological necrosis showed restricted diffusion and lower ADC values. For malignant pulmonary lesions, the ADC value of the lung cancers with necrosis was significantly lower than that of the lung cancers without necrosis.[30] Abscesses and thrombi are believed to impede the diffusivity of water molecules because of their hyperviscous nature.[31,32] Second, mucinous carcinomas were hypointense in DWI and had higher ADC values, which could be misdiagnosed as benign lesions in DWI.[30] Mucinous carcinomas have higher ADC values and lower DWI signal intensity than tubular adenocarcinoma in the anorectal region, because mucinous carcinomas have far lower cellularity than ordinary tubular adenocarcinoma.[33]

None of our patients were infected by histoplasmosis or coccidiosis. Indeed, there is low incidence of histoplasmosis and coccidiosis in Japan. The diagnostic effect of DWI is not clear in regions with high incidence of histoplasmosis or coccidiosis.

We have come to the conclusion that DWI can be used in place of PET-CT. DWI is an important tool in the evaluation of pathologic conditions in the lymph nodes and should be utilized during routine imaging.

ACKNOWLEDGMENT This study was supported partly by a Grant-in-Aid for Scientific Research from the Ministry of Education, Culture, Sports, Science and Technology, Japan (21591828). We are grateful to Mr. Masaru Takahashi and Mr. Keiya Hirata of the MRI Center, Kanazawa Medical University, for technical assistance.

DISCLOSURE The authors declare no conflict of interest.

REFERENCES

1. Dwamena BA, Sonnad SS, Angobaldo JO, Wahl RL. Metastases from non-small cell lung cancer. Mediastinal staging in the 1990s. Meta-analytic comparison of PET and CT. *Radiology*. 1999;213:530–6.
2. Toloza EM, Harpole L, McCrory DC. Noninvasive staging of non-small cell lung cancer. *Chest.* 2003;123:137S–46S.
3. Could MK, Kuschner WG, Rydzak CE, et al. Test performance of positron emission tomography and computed tomography for mediastinal staging in patients with non-small-cell lung cancer. *Ann Intern Med*. 2003;139:879–92.
4. Roberts PF, Follette DM, von Haag D, Park JA, Valk PE, Pounds TR, Hopkins DM. Factors associated with false-positive staging of lung cancer by positron emission tomography. *Ann Thorac Surg*. 2000;70:1154–9.
5. Le Bihan D, Breton E, Lallemand D, Aubin ML, Vignaud J, Laval-Jeantet M. Separation of diffusion and perfusion in intravoxel incoherent motion MR imaging. *Radiology.* 1988;168:497–505.
6. Tien RD, Felsberg GJ, Friedman H, Brown M, MacFall J. MR imaging of high-grade cerebral gliomas. Value of diffusion-weighted echoplanar pulse sequences. *AJR Am J Roentgenol.* 1994;162:671–77.
7. Sorensen AG, Buonanno FS, Gonzalez RG, et al. Hyperacute stroke. Evaluation with combined multisection diffusion-weighted and hemodynamically weighted echo-planar MR imaging. *Radiology.* 1996;199:391–401.
8. Schaefer PW, Grant PE, Gonzalez RG. Diffusion-weighted MR imaging of the brain. *Radiology.* 2000;217:331–45.
9. Szafer A, Zhong J, Gore JC. Theoretical model for water diffusion in tissues. *Magn Reson Med.* 1995;33:697–712.
10. Takahara T, Imai Y, Yamashita T, Yasuda S, Nasu S, Van Cauteren M. Diffusion weighted whole body imaging with background body signal suppression (DWIBS). Technical improvement using free breathing, STIR and high resolution 3D display. *Radiat Med.* 2004;22:275–82.
11. Nasu K, Kuroki Y, Kuroki S, Murakami K, Nawano S, Moriyama N. Diffusion-weighted single shot echo planar imaging of colorectal cancer using a sensitivity-encoding technique. *Jpn J Clin Oncol.* 2004;34:620–6.
12. Komori T, Narabayashi I, Matsumura K, et al. 2-fluorine-18 fluoro-2-deoxy-D-glucose positron emission tomography/ computed tomography versus whole-body diffusion-weighted MRI for detection of malignant lesions. Initial experience. *Ann Nucl Med.* 2007;21:209–15.
13. Nomori H, Mori T, Ikeda K, Kawanaka K, Shiraishi S, Katahira K, Yamashita Y. Diffusion-weighted magnetic resonance imaging can be used in place of positron emission tomography for N staging of non-small cell lung cancer with fewer false-positive results. *J Thorac Cardiovasc Surg.* 2008;135:816–22.
14. Mori T, Nomori H, Ikeda K, Kawanaka K, Shiraishi S, Katahira K, Yamashita Y. Diffusion-weighted magnetic resonance imaging for diagnosing malignant pulmonary nodules/masses. Comparison with positron emission tomography. *J Thorac Oncol.* 2008;3:358–64.
15. Usuda K, Zhao XT, Sagawa M, et al. Diffusion-weighted imaging is superior to PET in the detection and nodal assessment of lung cancers. *Ann Thorac Surg.* 2011;91:1689–95.
16. International Union Against Cancer. TNM classification of malignant tumours, 7th edn. New York: Wiley-Liss; 2009. p. 138–46.
17. Higashi K, Ueda Y, Seki H, et al. Fluorine-18-FDG PET imaging is negative in bronchioloalveolar lung carcinoma. *J Nucl Med.* 1998;39:1016–20.
18. Cheran SK, Nielsen ND, Patz EF. False-negative findings for primary lung tumors on FDG positron emission tomography. Staging and prognostic implications. *AJR Am J Roentgenol.* 2004;182:1129–32.
19. Satoh Y, Ichikawa T, Motosugi U, Kimura K, Sou H, Sano K, Araki T. Diagnosis of peritoneal dissemination. Comparison of 18F-DDG PET/CT, diffusion-weighted MRI, and contrast-enhanced MDCT. *AJR Am J Roentgenol.* 2011;196:447–53.
20. Goo JM, Im JG, Do KH, Yeo JS, Seo JB, Kim HY, Chung JK. Pulmonary tuberculoma evaluated by means of FDG PET. Findings in 10 cases. *Radiology.* 2000;216:117–21.
21. Nomori H, Watanabe K, Ohtsuka T, Naruke T, Suemasu K, Uno K. Evaluation of F-18 fluorodeoxyglucose (FDG) PET scanning for pulmonary nodules less than 3 cm in diameter, with special reference to the CT images. *Lung Cancer.* 2004;45:19–27.
22. Ohba Y, Nomori H, Mori T, et al. Is diffusion-weighted magnetic resonance imaging superior to positron emission tomography with fludeoxyglucose F 18 in imaging non-small cell lung cancer? *J Thorac Cardiovasc Surg.* 2009;138:439–45.
23. Tondo F, Saponaro A, Stecco A, Lombardi M, Casadio C, Carriero A. Role of diffusion-weighted imaging in the differential diagnosis of benign and malignant lesions of the chest-mediastinum. *Radiol Med.* 2011;116:720–33.
24. Yamamura J, Salomon G, Buchert R, et al. Magnetic resonance imaging of prostate cancer. Diffusion-weighted imaging in comparison with sextant biopsy. *J Comput Assist Tomogr.* 2011;35:223–8.

25. Fornasa F, Pinali L, Gasparini A, Toniolli E, Montemezzi S. Diffusion-weighted magnetic resonance imaging in focal breast lesions. Analysis of 78 cases with pathological correlation. *Radiol Med.* 2011;116:264–75.
26. Koike N, Cho A, Nasu K, Seto K, Nagaya S, Ohshima Y, Ohkohchi N. Role of diffusion-weighted magnetic resonance imaging in the differential diagnosis of focal hepatic lesions. *World J Gastroenterol.* 2009;15:5805–12.
27. Park HK, Jeon K, Koh WJ, et al. Occult nodal metastasis in patients with non-small cell lung cancer at clinical stage IA by PET/CT. *Resirology.* 2010;15:1179–84.
28. Bille A, Pelosi E, Skanjeti A, et al. Preoperative intrathoracic lymph node staging in patients with non-small-cell lung cancer. Accuracy of integrated positron emission tomography and computed tomography. *Eur J Cardio-thorac Surg.* 2009;36:440–5.
29. Kosucu P, Tekinbas C, Erol M, Sari A, Kavgaci H, Oztuna F, Ersöz S. Mediastinal lymph nodes. Assessment with diffusion-weighted MR imaging. *J Magn Reson Imaging.* 2009;30:292–7.
30. Usuda K, Sagawa M, Motono N, et al. Comparison of diffusion-weighted imaging and positron emission tomography-computed tomography in distinguishing malignant from benign pulmonary nodules and mass lesions. *Ann Surg Oncol.* (in submission).
31. Kwee TC, Takahara T, Ochiai R, et al. Complementary roles of whole-body diffusion-weighted MRI and ^{18}F-FDG PET. The state of the art and potential application. *J Nucl Med.* 2010:51:1549–58.
32. Desprechins B, Stadnik T, Koerts G, Shabana W, Breucq C, Osteaux M. Use of diffusion-weighted MR imaging in differential diagnosis between intracerebral necrotic tumors and cerebral abscesses. *Am J Neuroradiol.* 1999;20:1252–7.
33. Nasu K, Kuroki Y, Minami M. Diffusion-weighted imaging findings of mucinous carcinoma arising in the ano-rectal region. Comparison of apparent diffusion coefficient with that of tubular adenocarcinoma. *Jpn J Radiol.* 2012;30:120–7.